



# Structure, physical properties and fractal characteristics of the arc PVD coatings deposited onto the ceramics materials

**W. Kwaśny\***

Division of Material Processing Technology, Management and Computer Techniques in Materials Science, Institute of Engineering Materials and Biomaterials, Silesian University of Technology, ul. Konarskiego 18a, 44-100 Gliwice, Poland

\* Corresponding author: E-mail address: waldemar.kwasny@polsl.pl

Received in a revised form 29.09.2010

## ABSTRACT

**Purpose:** The goal of the presented study was to develop a methodology giving a possibility to predict functional properties of coatings obtained in the arc PVD process onto the ceramics materials, based on fractal and multi-fractal quantities describing their surface.

**Design/methodology/approach:** Effect of process type and deposition conditions on structure and shape of surface, as well as mechanical and service properties of the obtained coatings were determined. Methodology and detailed description of coatings topography obtained in the PVD process on ceramics materials, including use of the fractal- and multi-fractal geometry based on images obtained on the atomic forces microscope were worked out. Relationships between fractal- and multi-fractal quantities and their mechanical and service properties were determined.

**Findings:** The investigation results confirmed the feasibility to predict the service properties defined in the cutting ability test for coatings obtained in the arc PVD process, based on the surface fractal dimension  $D_s$  value for their surface topography.

**Research limitations/implications:** The geometrical features description of surfaces of the coatings obtained in the PVD processes.

**Practical implications:** Determining significant quantitative correlations between fractal quantities defining coatings' surfaces, as well as their service and/or mechanical properties provides the opportunity to predict their end-user properties.

**Originality/value:** Fractal and multifractal analysis gives possibility to characterise the extent of irregularities of the analysed surface in the quantitative way.

**Keywords:** Methodology of research; Computer assistance in the engineering tasks and scientific research; Fractal dimension; Multifractal spectrum

**Reference to this paper should be given in the following way:**

W. Kwaśny, Structure, physical properties and fractal characteristics of the arc PVD coatings deposited onto the ceramics materials, Archives of Computational Materials Science and Surface Engineering 2/4 (2010) 189-200.

## ENGINEERING MATERIALS PROPERTIES

## 1. Introduction

Topography of surface of many actual engineering materials, including CVD and PVD coatings, draws a self-similar feature [1-3], what allows to be applied to their description of the fractal analysis method. As surfaces of actual materials are never perfectly "smooth", so once adequately large enlargement of their fragments is applied, irregularities in the form of valleys and convexities appear. It can be noticed that for some materials, a degree of those irregularities is constant regardless of scale. It means that if analysed surface is smooth and regular, their fragments maintain this feature after being enlarged. When surface is irregular and rough, also its enlarged fragments look the same. It occurs like this, because additional details are disclosed which were not apparent earlier. Fractal geometry is a tool which allows characterizing degree of surface irregularities in qualitative and quantitative way when this value does not depend on scale. The basic fractal quantity that characterizes efficiency of space filling by surface and describes its shape is the surface fractal dimension -  $D_s$ . The fractal dimension  $D_s$ , being a real number in interval [2, 3] is a measure of irregularities and a degree of complexity of surface shape. Low value of fractal measure is characteristic for smooth surfaces, whereas high value describes surfaces of complex and complicated shape.

Practically, as early as the theory of fractals was established, B.B. Mandelbrot [4] indicated that, for description of the majority of actual objects (he chose distribution of copper deposits for example), application of the fractal formalism is insufficient. It results from a fact that actual objects are not homogenous, and because of that, it is impossible to describe geometrical features of objects of irregular shapes (except for the abstract mathematical constructions) with the help of one number – the fractal dimension. Surfaces of investigated engineering materials usually are not ideal self-similar objects, because that feature occurs only locally. Irregularities distribution changes depending on analysed fragment selection of a sample area. In some fragments, surfaces can be characterized by high irregularity, whereas they may reveal a more regular shape in the others. Mandelbrot has proposed to generalize a concept of the fractal set and replace it by a multi-fractal measure. The multi-fractal measure enables to characterize complex shapes, including surface, for which determined dimension adopts different values in different areas. Therefore, a multi-fractal analysis is an extension of the fractal method, enabling to characterize the geometrical features of actual surfaces in more complete and accurate way [2].

In contemporary science, the fractal and multi-fractal geometry found application, among other things, to investigate surface irregularities and to describe its shape. So far, fractal and multi-fractal features of surface have been determined for a number of materials, among which it is necessary to enumerate: metal materials [5] and their alloys [6], ceramic, polymeric and amorphous materials [7]. Besides, the fractals concept was used for description fractures surface morphology in 2D & 3D dimension for the sake of stereology [8]. As a result of amorphous samples tests, made of FeNiVSiB alloys, shown in [9] it is indicated that their resistance to fracture toughness proportional to a value of the fractal dimension of fracture topography. Application of electron microscopy enables to investigate

polymer-composite materials strengthens by mineral particles. The fractal analysis that has been conducted on the basis of obtained results facilitates a quantity description of quality scattering of mineral particles, thanks to application of numerical indicator connected with multi-fractal spectrum [11]. Serving the multi-fractal analysis, an attempt to describe the Portevin - Le Chatelier effect was undertaken (PLC) [12]. From a deformation curve, probability of plastic instability occurrence inside the investigated structure is determined, and a measure of a degree of material surface heterogeneity, in which plastic strain is found, was the fractal dimension. In the thesis [13], surface tests results are presented for materials remelted by laser. It is shown that materials remelted by a laser beam of higher energy are characterized by higher heterogeneity of surface, and over a specific character of multi-fractal spectrum describing it, energy of the laser beam has an impact. Received results show correlation between quantities describing a multi-fractal spectrum and changes about heterogeneity of coating in case of increase of the process time needed to deposit it.

Fractal and multi-fractal geometry also finds broad application in terms of characterizing and describing surface morphology of biomedical materials (biomaterials). Preparation of implants and coats for materials surface implantation in human organism's interior or used for prolonged contact with it (e.g. pacemakers and artificial heart valves, catheters, drains, surgical sutures) is for the present very intensively developing course of scientific research. Biomaterials, the most frequently used, include polymers, ceramic materials and some metals and their alloys. For their imaging, depending on the size of investigated areas, optical, confocal, atomic force, scanning or transmission microscopy is applied, and in order to assess the obtained results we mainly use methods for automatic image analysis, including the fractal analysis. In case of biomedical materials, used as implants, topography of their surface plays extraordinary important part in it. The fractal analysis application enables in this area to determine quantity parameters describing amplitude of irregularities on surface and a degree of their arrangement. A complementary approach, considering, except for roughness measurement, also the fractal dimension determining, has been practically used to optimize a process to obtain materials of demanded surface properties. In the field of ceramic materials investigation, used in medicine, researchers' efforts are focused upon elaboration of methods making a quantity assessment for applied materials porosity possible. The tests results [14] determine that the fractal is proportional to the ceramic materials porosity, and there is correlation between its value and water amount which can be absorbed by the material. It is determined that in case of the ceramic materials applied in dentistry, there is a dependence between hardness and the fractal dimension, moreover, the fractal geometry was used to monitor morphological changes of dental implants characterizing, including its application, the analyzed biomaterials consumption [15].

## 2. Material for studies

Studies are performed on:

- Multi-edge inserts made of oxide tool cermets  $Al_2O_3+ZrO_2$ ,
- Multi-edge inserts made of oxide tool cermets  $Al_2O_3+TiC$ ,

- Multi-edge inserts made of oxide tool cermets  $\text{Al}_2\text{O}_3+\text{SiC}$ ,
- Multi-edge inserts made of tool cermets  $\text{TiCN}+\text{TiC}+\text{TaC}+\text{Co}+\text{Ni}$  (T130A),
- Multi-edge inserts of tool cermets  $\text{TiCN}+\text{TiC}+\text{WC}+\text{TaC}+\text{Co}+\text{Ni}$  (CM).

Investigated ceramic tool materials are covered with single and multi-layer coatings in a process of cathodic arc evaporation - PVD process. Characteristics of investigated materials is presented in Table 1.

Table 1. Characteristics of the investigated coatings obtained in PVD process

Item	Material of substrate	Type of coating
1	$\text{Al}_2\text{O}_3+\text{ZrO}_2$	$\text{TiN}+(\text{Ti,Al,Si})\text{N}$
2	$\text{Al}_2\text{O}_3+\text{TiC}$	$\text{TiN}+(\text{Ti,Al,Si})\text{N}$
3	$\text{Al}_2\text{O}_3+\text{SiC}_{(w)}$	$\text{TiN}+(\text{Ti,Al,Si})\text{N}$
4	$\text{Al}_2\text{O}_3+\text{ZrO}_2$	TiN
5	$\text{Al}_2\text{O}_3+\text{TiC}$	TiN
6	$\text{Al}_2\text{O}_3+\text{SiC}_{(w)}$	TiN
7	$\text{Al}_2\text{O}_3+\text{ZrO}_2$	$\text{TiN}+\text{multi}(\text{Ti,Al,Si})\text{N}+\text{TiN}$
8	$\text{Al}_2\text{O}_3+\text{TiC}$	$\text{TiN}+\text{multi}(\text{Ti,Al,Si})\text{N}+\text{TiN}$
9	$\text{Al}_2\text{O}_3+\text{SiC}_{(w)}$	$\text{TiN}+\text{multi}(\text{Ti,Al,Si})\text{N}+\text{TiN}$
10	$\text{Al}_2\text{O}_3+\text{ZrO}_2$	(Ti,Al)N
11	$\text{Al}_2\text{O}_3+\text{TiC}$	(Ti,Al)N
12	$\text{Al}_2\text{O}_3+\text{SiC}_{(w)}$	(Ti,Al)N
13	$\text{Al}_2\text{O}_3+\text{ZrO}_2$	$\text{TiN}+(\text{Ti,Al,Si})\text{N}+(\text{Al,Si,Ti})\text{N}$
14	$\text{Al}_2\text{O}_3+\text{TiC}$	$\text{TiN}+(\text{Ti,Al,Si})\text{N}+(\text{Al,Si,Ti})\text{N}$
15	$\text{Al}_2\text{O}_3+\text{SiC}_{(w)}$	$\text{TiN}+(\text{Ti,Al,Si})\text{N}+(\text{Al,Si,Ti})\text{N}$
16	Cermet T130A	$\text{TiN}+(\text{Ti,Al,Si})\text{N}$
17	Cermet CM	$\text{TiN}+(\text{Ti,Al,Si})\text{N}$

### 3. Study methodology

Structure of generated coatings was observed at lateral fractures on a High Resolution Scanning Electron Microscope SUPRA 35, ZEISS Company.

Investigations for material surface topography of substrates and generated coatings are carried out in an exchanged scanning electron microscope and using a method of atomic force microscopy (AFM) on a unit of Nanoscope E made by Digital Instruments company. For each of analyzed surface, six measurements are made at scanning range of 5  $\mu\text{m}$ .

X-rays studies for the analyzed materials are carried out on X'Pert PRO system made by Panalytical Company using filter radiation of a cobalt anode lamp. A phase analysis of the analysed materials is carried out in Bragg-Brentano geometry (XRD) using a X'celerator strip detector, and in grazing incidence geometry (GIXRD) of primary beam using a collimator of parallel beam in front of a proportional detector.

In order to specify distribution of normal coatings towards a selected plane and to determine FRO (orientation distribution function of crystallites) acquired in PVD processes, not less than three pole figures were measured for each analysed sample made by a reflection method employing Euler's circle of diameter 187

mm in a range of samples inclination angle from zero to 75°. The FRO analysis of the analyzed materials was conducted with the help of procedures available in LaboTex 3.0 software using a discreet ADC method employing an iterative operator [16].

Measurements of stresses for the analyzed coatings were made by  $\sin^2\psi$  and/or  $g\text{-}\sin^2\psi$  technique depending on the investigated samples properties on the basis of PANalytical's X'Pert Stress Plus software. In the method of  $\sin^2\psi$ , based on diffraction lines displacement effect for different  $\psi$  angles, appearing in the conditions of stress of materials with crystalline structure, a silicon strip detector was used at the side of diffracted beam. Samples inclination angle  $\psi$  towards the primary beam was changed in the range of 0° - 75°. Moreover, measurements of stresses are made by a diffraction technique in grazing incidence geometry using a collimator of a parallel beam in front of the proportional detector.

Selection of incident angle of the primary beam ( $\alpha_x = 0,5^\circ; 1^\circ; 2^\circ; 3^\circ; 5^\circ; 7^\circ$ ) was mainly dependant on linear absorptivity and combination of the applied layers, but the effective X-rays penetration depth  $g$  is estimated on the basis of the following dependence:

$$g = \left( \frac{\mu}{\sin \mu} + \frac{\mu}{\sin(2\theta_{\{hkl\}} - \alpha_x)} \right)^{-1} \quad (1)$$

where:

$\mu$  – linear absorption of the X-rays,

$\alpha_x$  – incident angle of the primary beam.

Microhardness investigations for produced coatings and substrates hardness are conducted by means of an ultramicrohardness tester - DUH 202 manufactured by Shimadzu Co. using Vickers method at load of 0.07 N.

Assessments for coatings adhesion to the substrate's material were made by a drawing method on Revetest device manufactured by CSEM Co

Roughness investigations for the generated coatings and substrates surface were carried out on Stronic3 profile measurement gauge + Taylor-Hobson companies.  $R_a$  quantity is adopted as a value, which determined the surface roughness in accordance with PN-EN ISO 4287.

Plates life without coatings and with deposited coatings are determined on the basis of technological cutting test in room temperature. Cutting ability test for investigated materials is made as a continuous turning method at PDF D180 lathe without cutting fluids. The material subjected to machining was grey cast iron EN-GJL-250 of hardness approx. 215 HBW. Life of plates is determined based on wear bandwidth measurements upon flank face, measuring a mean bandwidth wear VB after machine cutting in specified period of time. Cutting tests were stopped, when VB value exceeded an assumed criterion ( $\text{VB} = 0.3 \text{ mm}$ ), both for uncovered tools and deposited coatings tools. VB measurements with an accuracy of up to 0,01 mm were made employing a Carl Zeiss Jena light microscope.

Indication of the fractal dimension and the multi-fractal analysis for investigated materials is carried out on the basis of optical measurements in atomic force microscope AFM, being grounded on projective covering method [17].

The measurements, which are carried out, using an atomic force microscope AFM enabled furthermore, indication of a quantity determined by the author as  $R_{2D}$  and characterizing roughness for analysed sample surface.  $R_{2D}$  roughness is determined in two stages. In the first one, each set of measurements results for the  $h_i$  sample height is approximated by the regression plane of  $H(x, y)$ , for which a sum of squares of the distance from experimental data is minimal, and then, a roughness quantity value  $R_{2D}$  is determined for the analyzed sample surface on the ground of a dependency:

$$R_{2D} = \left[ \frac{\sum_i (h_i - H_i)^2}{N_s} \right]^{\frac{1}{2}} \quad (2)$$

where:

$N_s$  – number of measuring points,

$h_i$  – sample height at  $i$  point,

$H_i$  – value of  $H(x, y)$  at  $i$  point.

Application of the above procedure eliminated influence of sample inclination (levelling error) over an acquired value of calculated quantity.

To verify significance of the product-moment correlation coefficients of the obtained results in mechanical, applicable and fractal studies,  $t$  statistics is used being subject to Student's distribution with a number of independent variables equals  $n - 2$ , where  $n$  is a number of measurements taken into account. Analyses were performed at the level of significance  $\alpha_{stat}=0.05$ . Empirical value for the test statistics  $t$  was determined in accordance with a formula:

$$t = \frac{r}{\sqrt{1-r^2}} \sqrt{n-2} \quad (3)$$

where  $r$  is an empirical Pearson product-moment correlation coefficient, based on a random sample. The symbol  $t_{kryt}$  standing

for a critical value, read out of tables for the test statistics distribution. Decision about a possible null hypothesis rejection (lack of correlations), was taken on the ground of the result for empirical value comparison of the test statistics with a critical value, read out from distribution tables of the test statistics. If  $|t| > t_{kryt}$ , the null hypothesis on lack of correlations was rejected as statistically less probable and the alternative hypothesis on correlations significance was accepted.

#### 4. Investigations results and discussion

As a result of factographic investigations performed on a scanning electron microscope for the analysed PVD coatings, it was found that the deposited coatings determine single, double, or multilayer structure depending on applied system of layers, and particular layers are uniformly deposited and tightly adhere to each other as well as to the substrate's material. Structure of particular layers depends on substrate's material and a type as well as conditions of process. Observations of surface topography for the analysed coatings using scanning microscopy demonstrate that the observed characteristic columns endings located on surface, forming appropriate coatings, have a shape of cones, polyhedrons or craters. However, it is difficult unequivocally to indicate differences among particular coatings in terms of quality and quantity on the basis of observations of the received topography images for the analysed surfaces (Fig. 1).

The applied method of X-ray qualitative phase analysis carried out in Bragg-Brentano geometry confirms occurrence of appropriate phases in the investigated substrates and coating materials. Some of identified reflexes on analysed diffraction patterns are moved towards lower or higher angles of reflection as well as their intensity differ from values given in JCPDS card files, what may indicate on occurrence of texture as well as of compressive or tensile, internal stresses in the investigated coatings – a fact one can come across frequently in coatings deposited by the PVD and CVD [18] technique. For the sake of reflexes overlapping of material substrate and coating/coatings, as

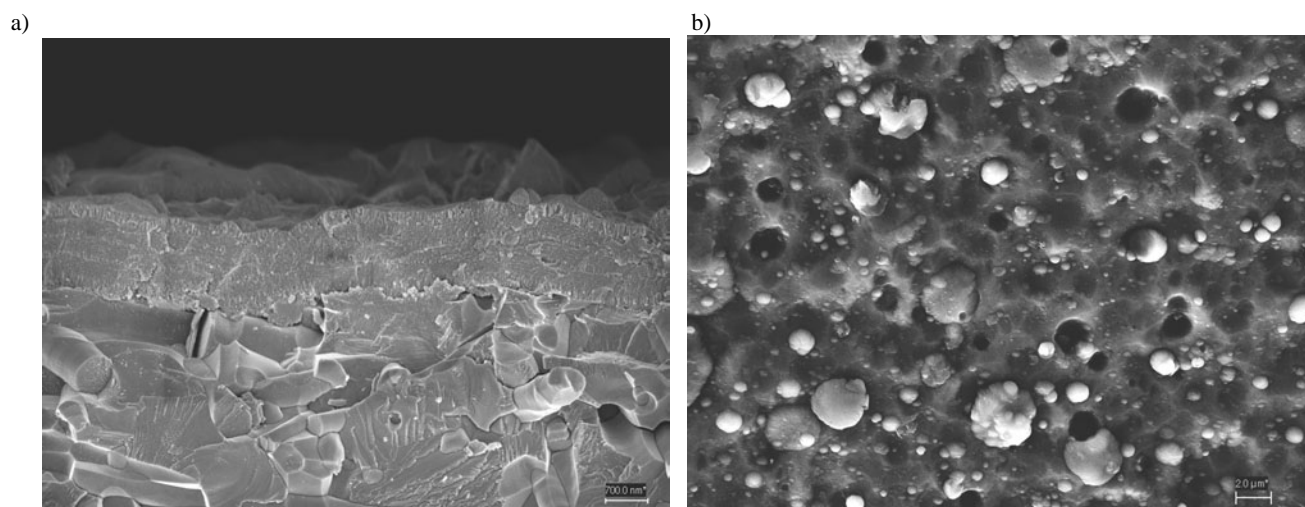


Fig. 1. a) Brittle fracture of a coating  $TiN+multi(Ti,Al,Si)N+TiN$  acquired on a substrate made of tool ceramics  $Al_2O_3+SiC$  in the arc PVD process and b) its image corresponding to topography of surface (SE detector)

well as their intensity, making sometimes the analysis of obtained results more difficult; and in order to acquire more accurate information from subsequent layers of the analyzed materials, additional technique of diffraction is applied at grazing incidence geometry (GIXRD), for the primary X-rays beam using a parallel beam collimator in front of proportional detector. Thanks to the possibility to register the diffraction patterns at low incidence angles of the primary beam onto the test piece surface, one can obtain the diffraction lines from thin layers due to volume growth of the material participating in diffraction and acquiring information on the changing phase composition at different depths of the examined material – which do not exceed the rays beam penetration depth when their incident angle is perpendicular to the test piece. Carried out investigations at such assumptions conform the right sequence of layers in analyzed coatings.

Texture analysis for investigated coatings is carried out by a reflexion method. Concentric distribution of pole figures intensity changing along with a beam of those figures indicates occurrence of axial component texture of coatings acquired in the arc PVD process. Calculations of volume fractions for texture components were carried out using integration of those components in FRO space subjected to transformation. In calculations of volume fractions, in identified texture components, angle broadening is taken into account ( $\Delta\Phi$ ,  $\Delta\phi_1$ ,  $\Delta\phi_2$ ), which is situated in the range of 10-15°. In case of coatings obtained in the arc PVD process, for the sake of overlapping reflexes, in most cases, of substrate and coating/coatings material, the full FRO analysis was not succeeded for the applied symmetrical Bragg-Brentano geometry of pole figures measurement, except for TiN coating obtained on substrate made of tool ceramics -  $\text{Al}_2\text{O}_3+\text{SiC}$ , in which volume fraction of the distinguished component  $\langle 111 \rangle$  is approx. 46% (Fig. 2). The analysis of texture made for coatings obtained in the arc PVD process allows stating, based on qualitative analysis of recorded single pole figures, that independently on substrate's material, in the following coatings TiN, TiN+(Ti,Al,Si)N+(Al,Si,Ti)N, TiN+(Ti,Al,Si)N, TiN+multi(Ti,Al,Si)N+TiN the

distinguished plane of increase is a plane of  $\{111\}$  family, whereas, in case of (Ti,Al)N coatings the texture of deposited layers is very weak. So that deposited coating on a tool could properly fulfil its task, it has to be characterized by suitable usable properties determined by numerous factors, among which the following should be specified: appropriate structure, chemical and phase composition, proper hardness and thickness, and above all, high adhesion to substrate's material. Specific nature of damages being responsible for fractions initiation, observed by means of a scanning microscope at the edge of scratch-coating depends on a type of process and a combination of the applied layers, and the following might be mainly enumerated: spallings formation on the edges in the shape of tiny craters, that in some cases are related to local delamination of a coating's fragment, conformal cracks induced by tension, undergoing single scaling, periodical delamination and one and two-sided spallings, as well as local stratification, and the following, as a consequence, displacement of torn fragments of the coating. Obtained outcomes of adhesion assessment depend on a type of process and applied layers, their thickness, chemical and phase composition, and also on material, upon which they were produced, what consequently has an impact on stresses value in the analysed coatings.

Stresses' measurements of the analyzed materials are performed by two methods, and obtained results are presented in Table 2. Stresses' measurements by  $\sin^2\psi$  method are made for three  $\varphi$  angles of samples arrangement towards an initial configuration, in which goniometer axis was in two opposite directions continuously ( $\varphi = 90^\circ$  &  $270^\circ$ ,  $\varphi = 150^\circ$  &  $330^\circ$ ,  $\varphi = 210^\circ$  &  $30^\circ$ ). Applying this geometry of measurement enables to observe changes of state of stress for chosen directions of investigated material and to determine its highest value.

In case of studying multi-layer coatings and/or coatings of phase composition close to the substrate's material, applying this geometry of measurement not always guarantees reception of correct results of measurements as a result of particular components reflexes overlapping of the investigated materials.

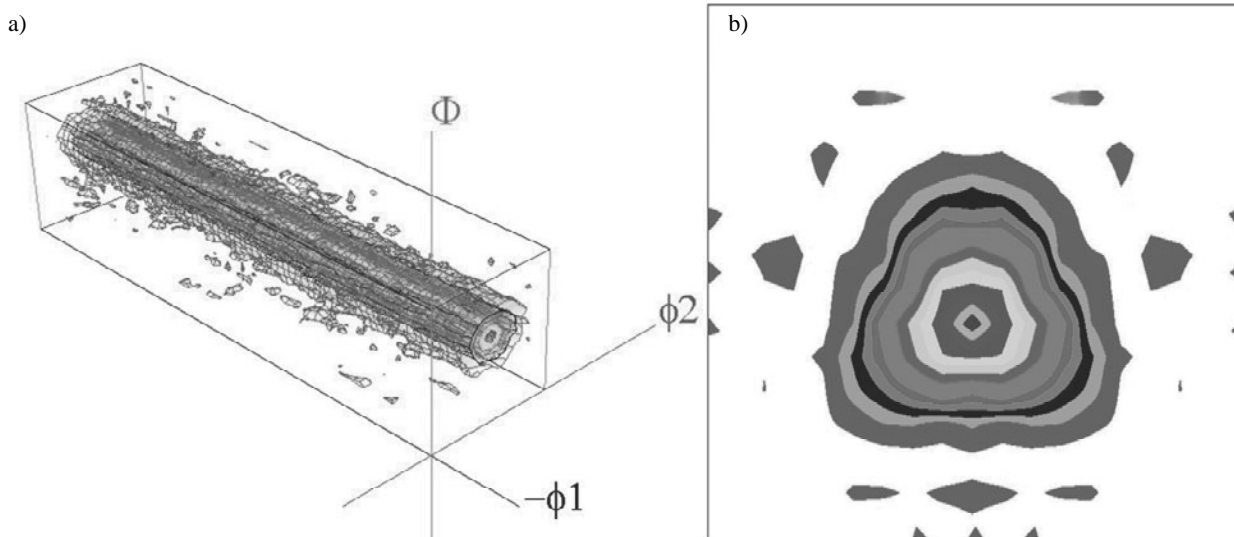


Fig. 2. Distribution function of coating orientation TiN obtained in the arc PVD process on the basis of tool ceramics  $\text{Al}_2\text{O}_3+\text{SiC}$   
a) 3D view FRO, b) FRO determined on the basis of pole figures subjected to symmetrisation (section acc. to  $\varphi_1$ )

Table 2.

Results of stresses' measurements of coatings obtained in the arc PVD process by  $\sin^2\psi$  and  $g\text{-}\sin^2\psi$  methods

Substrate's material	Type of coating	Coating thickness [μm]	Method $\sin^2\psi$ [MPa]	Method $g\text{-}\sin^2\psi$ [MPa]
Al <sub>2</sub> O <sub>3</sub> +ZrO <sub>2</sub>	TiN+(Ti,Al,Si)N	1.9	-	-461±45
Al <sub>2</sub> O <sub>3</sub> + TiC	TiN+(Ti,Al,Si)N	2.4	-	-651±74
Al <sub>2</sub> O <sub>3</sub> + SiC <sub>(w)</sub>	TiN+(Ti,Al,Si)N	2.5	-	-672±62
Al <sub>2</sub> O <sub>3</sub> +ZrO <sub>2</sub>	TiN	1.1	-	-251±56
Al <sub>2</sub> O <sub>3</sub> + TiC	TiN	1.3	-	-221±71
Al <sub>2</sub> O <sub>3</sub> + SiC <sub>(w)</sub>	TiN	1.1	-298±46	-311±75
Al <sub>2</sub> O <sub>3</sub> +ZrO <sub>2</sub>	TiN+multi(Ti,Al,Si)N+TiN	2.3	-	-455±54
Al <sub>2</sub> O <sub>3</sub> + TiC	TiN+multi(Ti,Al,Si)N+TiN	2.7	-	-621±63
Al <sub>2</sub> O <sub>3</sub> + SiC <sub>(w)</sub>	TiN+multi(Ti,Al,Si)N+TiN	2.8	-	-551±59
Al <sub>2</sub> O <sub>3</sub> +ZrO <sub>2</sub>	(Ti,A)N	2.2	-791±29	-822±34
Al <sub>2</sub> O <sub>3</sub> + TiC	(Ti,A)N	2.2	-798±27	-893±29
Al <sub>2</sub> O <sub>3</sub> + SiC <sub>(w)</sub>	(Ti,A)N	2.1	-1144±24	-1128±32
Al <sub>2</sub> O <sub>3</sub> +ZrO <sub>2</sub>	TiN+(Ti,Al,Si)N+(Al,Si,Ti)N	2.2	-	-284±51
Al <sub>2</sub> O <sub>3</sub> + TiC	TiN+(Ti,Al,Si)N+(Al,Si,Ti)N	2.2	-	-509±63
Al <sub>2</sub> O <sub>3</sub> + SiC <sub>(w)</sub>	TiN+(Ti,Al,Si)N+(Al,Si,Ti)N	2.5	-	-231±58
Cermetal T130A	TiN+(Ti,Al,Si)N	4.6	-	-1070±42
Cermetal CM	TiN+(Ti,Al,Si)N	4.5	-	-1211±39

Because of this, measurements of the analyzed coatings stresses are conducted additionally by a method of  $g\text{-}\sin^2\psi$ . The method  $g\text{-}\sin^2\psi$  defining stresses based on geometry of a constant incidence angle was proposed by Van Hacker [19], Quaeys and Knuyt [20], and then, it was expanded by Skrzypek. Finally, algorithm for calculations of stresses was applied by Skrzypek and Baczański [21, 22]. The method of  $g\text{-}\sin^2\psi$  is characterized by the use of many diffraction lines from planes {hkl} in contradiction to a classical method of  $\sin^2\psi$ , using one diffraction line. The main advantage of the method  $g\text{-}\sin^2\psi$  in reference to the classical method  $\sin^2\psi$  measuring stresses, where we are engaged in variable, effective depth of penetration of X-rays radiation into the investigated material, it is almost a constant value for a fixed value  $\alpha_x$ , which can be changed by incidence angle or selection of different type of radiation. Moreover, in this method, changing reflexes {hkl} for a crystallographic plane are simultaneously used in a measuring procedure to determine stresses and the method can be easily applied for changing geometries of measurement [21].

Each time measurements of stresses were carried out upon external coating, and as far as it was possible, depending on a type of substrate's material, properties and configurations of the applied layers, in a coating adhering to it, using one or two non-destructive methods to measure this size. Results of the performed studies for internal macro-stresses of the analyzed coatings indicate a correlation between a size of stresses and hardness as well as adhesion to substrates of the investigated coatings (Fig. 3). A value of adhesion to substrate's material from stresses occurring in coatings can be defined by the following analytical  $y = -0.0691x + 26.3277$  for the arc process (correlation coefficient  $r = 0.913$ , the empirical test statistics value  $t = 8.683$ , critical value  $t_{\text{kr}} = 2.131$ ) (Fig. 4). Phase and chemical composition, conditions and type of process as well as substrate's material and combination of the applied layers and texture influence on microhardness of the investigated coatings. Based on performed

studies for cutting ability, it was found that coatings' deposition in the PVD processes on ceramic tool materials causes increase their frictional wear resistance, what directly influences over extension of a cutting tool life. The presented results indicate that wear rate reduction of a surface cutting plates rank along with deposited coatings depends on their structure and topography of surface, phase and chemical composition, mechanical properties and substrate's material, upon which they have been obtained. In the Table 3, measurements results of mechanical and operational properties are presented for coatings acquired in the arc PVD process. As a result of a metallographic analysis, conducted on a scanning electron microscope, it was found that the most frequently occurring types of tribological damages, identified on investigated materials are mechanical and frictional damages, as well as thermal cracks of the surface flank, crater forming on surface of attack and a chip build-up on a cutting edge [23].

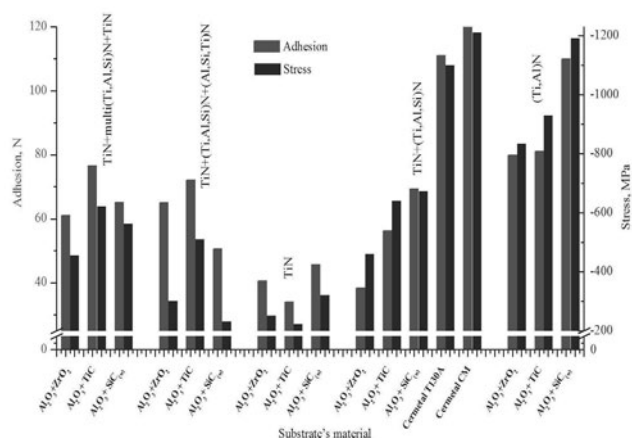


Fig. 3. Adhesion and stresses dependence on substrate's material for coatings obtained in the arc PVD process

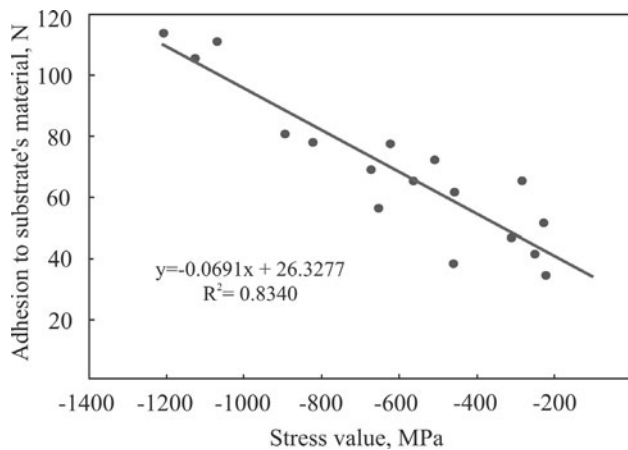


Fig. 4. Adhesion and stresses dependence on substrate's material for coatings obtained in the arc PVD process

## 5. Fractal and multi-fractal analysis of the investigated coatings

In the herewith evaluation to determine the fractal dimension of coatings surface obtained in the PVD processes, a modified method for projective covering (PCM) was applied [17]. The PCM method was evaluated at the end of the last century and used for determining the fractal dimension of surface of rocks, and then, it was used many a time in studies for surface of diverse engineering materials [1-3, 5, 8-12].

Fractal and multi-fractal analysis of the investigated coatings obtained in the arc PVD process were carried out based on results acquired on atomic force microscope AFM. Initial measurements were made in measuring ranges equal 1, 2, 5 and 10  $\mu\text{m}$ , however, not all analyses confirmed fractal properties of the analysed coatings. Results for internal studies, which were presented by the author in points [1-3], allow to find that considering possibility to compare results for coatings, the right scanning range is 5  $\mu\text{m}$ . Three dimensional images of coatings surface topography obtained based on data from measurements made by means of on AFM microscopes are precious source of information on shape of surface, however, their interpretation and comparison are difficult, subjective and often lead to false conclusions. Appearance of those graphs, in a large degree, depends on the way they are presented (applied colours and their intensity, perspective, and the like) and applied scale in z axis. Simultaneously, applying a rule that for all compared samples in z axis the same unit appears, especially a unit equal to a unit occurring in x and y axes, make the graphs more illegible. For the sake of images of coatings surface topography received based on data coming from measurements made on AFM microscopes, they can only give an idea about shape of surface, but they should not be used in highly advanced analyses.

Making measurements on the AFM microscope and getting digital recording of topography of the analyzed surfaces created a possibility to determine two-dimensional quantity of roughness  $R_{2D}$ , which in comparison with classical quantities determined along one segment, enables to obtain more representative values.

The roughness quantity is a commonly used value defining shape of surface, and first of all, it should be considered when comparing and assessing the shape of coatings.

$R_{2D}$  roughness determined based on measurements made by the AFM microscope is an informing quantity on, in what degree the analyzed area differs from the flat surface, but it does not indicate what made this difference, whose source might be of two different factors:

- Surface waviness (irregularity occurrence of high amplitude),
- Appropriate roughness (densely arranged irregularity occurrence of low amplitude).

The fractal analysis enables to differentiate those factors, and additionally, thanks to determining the multi-fractal spectrum, to assess homogeneity of the analysed objects. The next stages of the fractal analysis cover:

- Bilogarithmic performance,
- Auxiliary plot performance indicating correct selection of the fractal range,
- Determining the surface fractal dimension  $D_s$ ,
- Determining the multi-fractal spectrum and defining its parameters.

Points arrangement on the bilogarithmic plot is defined by a degree of an analysed surface development, and simultaneously it indicates factors which have influence on it: surface waviness or appropriate roughness. On the ground of the bilogarithmic plot also fractality of the analysed set of data is assessed. Performing an auxiliary plot facilitates the right selection of the fractality range or taking a decision that the analysed set of data is not a fractal object. Analysing a shape of the multi-fractal spectrum, it can be concluded on homogeneity of analysed surfaces. Homogenous surfaces, whose particular fragments do not differ among themselves, are characterized by a narrow spectrum (small difference  $\alpha_{\text{max}} - \alpha_{\text{min}}$ ), which can be broadened, if a shape of the analysed surface will be more irregular and differentiated in various areas. For the sake of the applied methodology determining the multi-fractal spectrum in the analyzed coatings, it is assumed that its maximum appears for  $\alpha = 2$ . As values  $\alpha < 2$  correspond to probabilities of low values and simultaneously to irregularities of low amplitude so, broadening the multi-fractal spectrum from the left side is characteristic for inhomogeneous surfaces containing tiny grains.

Analogically, broadening the spectrum from the right side (for values  $\alpha > 2$ ) it proves that big grains and/or flat areas occur. A positive difference for the spectrum arms height  $\Delta f = f(\alpha_{\text{max}}) - f(\alpha_{\text{min}}) > 0$  proves that in the analysed surface, tiny grains dominate, otherwise ( $\Delta f < 0$ ) high irregularities prevail, defined by high value of probability. Although the multi-fractal spectrum bandwidth is not commonly bound with homogeneity of analysed surface, interpretation of its shape is not unequivocal. The other factors (e.g. roughness, fractal dimension) influence additionally on values describing appearance of the multi-fractal spectrum. Therefore, values analysing that define a shape of the multi-fractal spectrum received for coatings' surface differed by simultaneously chemical and phase composition, conditions and a type of their obtaining process and substrate's material, on which they were produced is not justified. Problems related to interpretations about shape of the multi-fractal spectrum demand further intensive investigations, nevertheless, still today one can indicate some practical applications, e.g. for quality control and

Table 3.

Results of mechanical and operational measurements for substrates' material as well as coating obtained in the arc PVD process

Substrate's material	Type of coating	Roughness $R_a$ [ $\mu\text{m}$ ]	Microhardness $HV_{0.05}$	Adhesion N	Operational properties	
					Tool life T (min)	Increase (%)
$\text{Al}_2\text{O}_3+\text{ZrO}_2$	TiN+(Ti,Al,Si)N	0.43	2200	38.3	14	27
$\text{Al}_2\text{O}_3+\text{TiC}$	TiN+(Ti,Al,Si)N	0.37	2530	56.2	18.5	30
$\text{Al}_2\text{O}_3+\text{SiC}_{(w)}$	TiN+(Ti,Al,Si)N	0.37	2300	69.4	20	11
$\text{Al}_2\text{O}_3+\text{ZrO}_2$	TiN	0.41	2300	40.6	12.5	14
$\text{Al}_2\text{O}_3+\text{TiC}$	TiN	0.21	2400	33.8	13.5	0
$\text{Al}_2\text{O}_3+\text{SiC}_{(w)}$	TiN	0.31	2670	45.7	25	39
$\text{Al}_2\text{O}_3+\text{ZrO}_2$	TiN+multi(Ti,Al,Si)N +TiN	0.37	3700	61.9	14.5	32
$\text{Al}_2\text{O}_3+\text{TiC}$	TiN+multi(Ti,Al,Si)N +TiN	0.27	3950	76.6	21.5	59
$\text{Al}_2\text{O}_3+\text{SiC}_{(w)}$	TiN+multi(Ti,Al,Si)N +TiN	0.39	3800	66.1	28	56
$\text{Al}_2\text{O}_3+\text{ZrO}_2$	(Ti,A)IN	0.23	3200	78.2	16	45
$\text{Al}_2\text{O}_3+\text{TiC}$	(Ti,A)IN	0.12	3100	79.6	17	26
$\text{Al}_2\text{O}_3+\text{SiC}_{(w)}$	(Ti,A)IN	0.26	3300	104.6	31	72
$\text{Al}_2\text{O}_3+\text{ZrO}_2$	TiN+(Ti,Al,Si)N+(Al,Si,Ti)N	0.39	2150	65.3	15	36
$\text{Al}_2\text{O}_3+\text{TiC}$	TiN+(Ti,Al,Si)N+(Al,Si,Ti)N	0.24	2950	72.2	19	41
$\text{Al}_2\text{O}_3+\text{SiC}_{(w)}$	TiN+(Ti,Al,Si)N+(Al,Si,Ti)N	0.32	2450	50.6	24	33
Cermetal T130A	TiN+(Ti,Al,Si)N	0.36	3350	111.1	26.5	76
Cermetal CM	TiN+(Ti,Al,Si)N	0.23	3300	114.8	29.5	73
Cermetal T130A	-	0.21	2490	-	15	-
Cermetal CM	-	0.37	2450	-	17	-
$\text{Si}_3\text{N}_4$	-	0.08	1870	-	12	-
$\text{Al}_2\text{O}_3+\text{ZrO}_2$	-	0.21	1850	-	11	-
$\text{Al}_2\text{O}_3+\text{TiC}$	-	0.09	1970	-	13.5	-
$\text{Al}_2\text{O}_3+\text{SiC}_{(w)}$	-	0.26	1870	-	18	-

repeatability of coatings' deposition process. Each  $\Delta\alpha$  value increase, above or below a certain defined critical value for a given process will be a signal informing about instability of deposition conditions. In case of surface received in conditions differing with one factor change, the multi-fractal analysis can be used to assess its influence on topography of obtained coatings. Quantities for the fractal and multi-fractal analysis and for the quantity value  $R_{2D}$  of the analysed coatings are presented in Table 4. On the basis of carried out analyses it can be found that all considered coatings, independently on type of their manufacturing process and the applied substrate's material, show fractal character of surface, what is proved by linear, in defined ranges, the bilogarithmic graphs used for determining the fractal dimension  $D_s$  (Fig. 5).

Analysing the received results for coatings acquired in the arc PVD process it was found that the fractal dimension value is situated within 2.006-2.252, whereas roughness is defined by  $R_{2D}$  quantity within 0.037 to 0.564  $\mu\text{m}$  (Table 4).

Surface topography images and results of the fractal and multi-fractal analysis for TiN+multi(Ti,Al,Si)N+TiN coatings

obtained in the arc PVD process on a substrate made of tool ceramics  $\text{Al}_2\text{O}_3+\text{TiC}$  is presented in Figure 5.

In Figure 6 the obtained results are presented for the fractal dimension values and operational properties depending on substrates' materials, including a value of the quantity  $\Delta\alpha$ . In the event of coatings obtained in the arc PVD process it was observed a positive correlation between the fractal dimension value and tool life increase (correlation coefficient  $r=0.601$ , the empirical test statistics value  $t=2.914$ , critical value  $t_{kryt}=2.131$ ) (Fig. 6).

Low value of correlation coefficient of operational properties and fractal quantities ( $r=0.6011$ ) reflects inhomogeneity of coatings on the basis of titanium nitride, obtained in the arc PVD process, defined by high quantity of  $\Delta\alpha$ . Coatings obtained in the arc PVD process are characterized by significantly wider range of the fractal dimension values than the other coatings obtained in the other processes. Considering results of measurements corresponding to coatings defined by low fractal dimension value ( $D_s < 2.1$ ), high value of correlation coefficient between the fractal dimension value and operational properties is obtained (correlation coefficient  $r=0.7599$ ,  $t=3.6977$ ,  $t_{kryt}=2.2281$ ) (Fig. 7).

Table 4. The fractal and multi-fractal analysis results and  $R_{2D}$  values for coatings obtained in the arc PVD process and a substrate made of tool oxide ceramics and cermets

Substrate's material	Type of coating	$R_{2D}$ [ $\mu\text{m}$ ]	$D_s$	$\alpha_{\min}$	$\alpha_{\max}$	$\Delta\alpha$	$f(\alpha_{\max})$	$f(\alpha_{\min})$
$\text{Al}_2\text{O}_3+\text{ZrO}_2$	TiN+(Ti,Al,Si)N	0.408±0.033	2.029±0.003	1.637±0.038	2.039±0.005	0.403±0.038	0.231±0.025	1.772±0.025
$\text{Al}_2\text{O}_3+\text{TiC}$	TiN+(Ti,Al,Si)N	0.095±0.012	2.027±0.003	1.740±0.026	2.008±0.001	0.268±0.026	0.004±0.031	1.947±0.009
$\text{Al}_2\text{O}_3+\text{SiC}_{(w)}$	TiN+(Ti,Al,Si)N	0.184±0.023	2.016±0.002	1.651±0.067	2.025±0.003	0.375±0.067	0.216±0.029	1.875±0.014
$\text{Al}_2\text{O}_3+\text{ZrO}_2$	TiN	0.133±0.017	2.018±0.002	1.807±0.021	2.014±0.001	0.207±0.021	0.006±0.043	1.897±0.016
$\text{Al}_2\text{O}_3+\text{TiC}$	TiN	0.037±0.005	2.006±0.001	1.865±0.024	2.004±0.001	0.139±0.024	0.003±0.003	1.963±0.005
$\text{Al}_2\text{O}_3+\text{SiC}_{(w)}$	TiN	0.564±0.054	2.122±0.018	1.532±0.057	2.118±0.019	0.586±0.060	0.216±0.033	1.764±0.033
$\text{Al}_2\text{O}_3+\text{ZrO}_2$	TiN+multi(Ti,Al,Si)N+TiN	0.087±0.009	2.019±0.005	1.846±0.016	2.013±0.003	0.167±0.016	0.284±0.051	1.897±0.019
$\text{Al}_2\text{O}_3+\text{TiC}$	TiN+multi(Ti,Al,Si)N+TiN	0.470±0.044	2.252±0.036	1.645±0.043	2.147±0.021	0.502±0.048	0.190±0.022	1.588±0.051
$\text{Al}_2\text{O}_3+\text{SiC}_{(w)}$	TiN+multi(Ti,Al,Si)N+TiN	0.440±0.037	2.128±0.022	1.530±0.081	2.091±0.014	0.561±0.082	0.182±0.026	1.735±0.027
$\text{Al}_2\text{O}_3+\text{ZrO}_2$	(Ti,Al)N	0.260±0.029	2.032±0.004	1.788±0.022	2.026±0.004	0.238±0.022	0.280±0.031	1.862±0.015
$\text{Al}_2\text{O}_3+\text{TiC}$	(Ti,Al)N	0.082±0.007	2.014±0.002	1.779±0.029	2.014±0.002	0.236±0.029	0.003±0.042	1.900±0.018
$\text{Al}_2\text{O}_3+\text{SiC}_{(w)}$	(Ti,Al)N	0.351±0.031	2.045±0.005	1.745±0.029	2.032±0.003	0.287±0.029	0.241±0.029	1.948±0.006
$\text{Al}_2\text{O}_3+\text{ZrO}_2$	TiN+(Ti,Al,Si)N+(Al,Si,Ti)N	0.261±0.025	2.034±0.004	1.612±0.054	2.0438±0.008	0.431±0.055	0.0113±0.002	1.800±0.034
$\text{Al}_2\text{O}_3+\text{TiC}$	TiN+(Ti,Al,Si)N+(Al,Si,Ti)N	0.236±0.019	2.060±0.008	1.642±0.061	2.038±0.004	0.396±0.061	0.092±0.011	1.823±0.019
$\text{Al}_2\text{O}_3+\text{SiC}_{(w)}$	TiN+(Ti,Al,Si)N+(Al,Si,Ti)N	0.237±0.025	2.029±0.003	1.573±0.049	2.031±0.003	0.458±0.049	0.311±0.039	1.888±0.021
Cermet Ti30A	TiN+(Ti,Al,Si)N	0.409±0.037	2.100±0.009	1.607±0.089	2.078±0.012	0.472±0.090	0.141±0.002	1.778±0.051
Cermet CM	TiN+(Ti,Al,Si)N	0.306±0.041	2.101±0.007	1.541±0.099	2.074±0.011	0.532±0.103	0.228±0.012	1.744±0.031
$\text{Al}_2\text{O}_3+\text{ZrO}_2$	-	0.060±0.006	2.009±0.001	1.818±0.019	2.007±0.001	0.190±0.019	0.001±0.029	1.945±0.006
$\text{Al}_2\text{O}_3+\text{TiC}$	-	0.033±0.003	2.009±0.001	1.831±0.023	2.006±0.001	0.175±0.023	0.004±0.014	1.951±0.007
$\text{Al}_2\text{O}_3+\text{SiC}_{(w)}$	-	0.043±0.004	2.008±0.001	1.828±0.021	2.006±0.001	0.178±0.021	0.002±0.039	1.960±0.008
Cermet Ti30A	-	0.180±0.021	2.153±0.021	1.483±0.078	2.131±0.015	0.648±0.079	0.009±0.018	1.533±0.083
Cermet CM	-	0.412±0.044	2.164±0.016	1.671±0.043	2.142±0.022	0.472±0.048	0.329±0.036	1.586±0.042

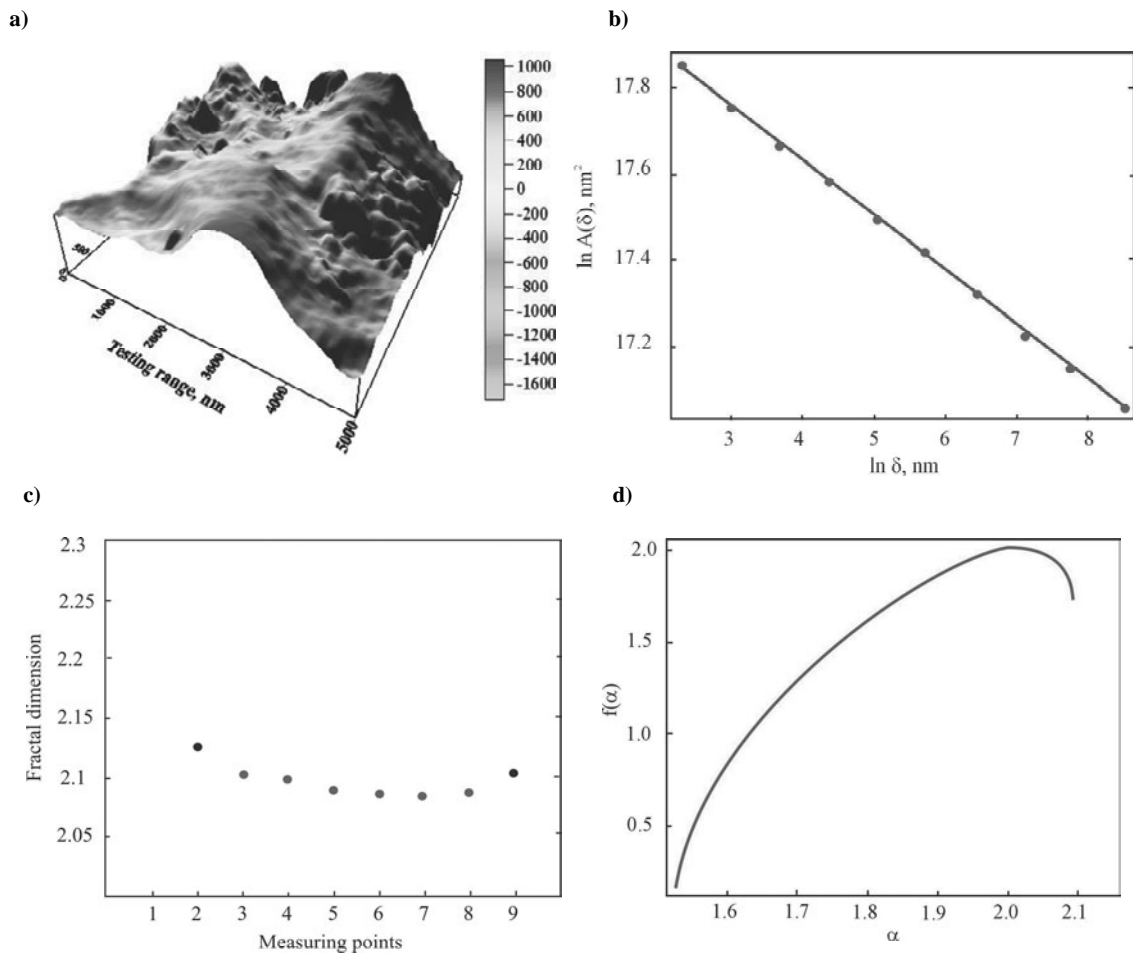


Fig. 5. a) Image of the TiN+multi(Ti,Al,Si)N+TiN coating surface obtained in the arc PVD process on the  $\text{Al}_2\text{O}_3+\text{TiC}$  (AFM, 5  $\mu\text{m}$ ) tool ceramics substrate b) bilogarithmic dependence of the approximated area size of the analysed surface on the mesh size used for its determination c) auxiliary diagram indicating the correct points selection on the bilogarithmic plot, and d) multi-fractal spectrum of the analysed coating surface

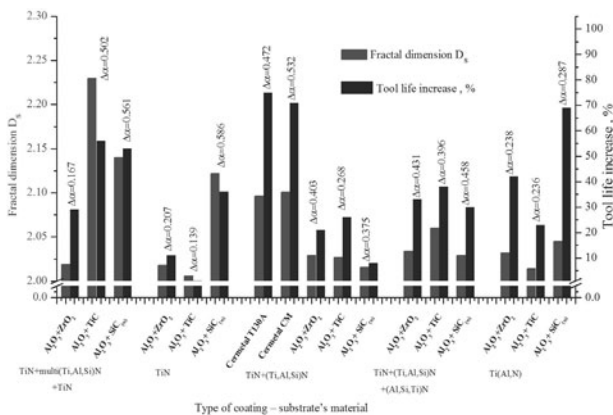


Fig. 6. Comparison of received results for the fractal dimension values  $D_s$ ,  $\Delta\alpha$  and operational properties of coatings obtained in the arc PVD process

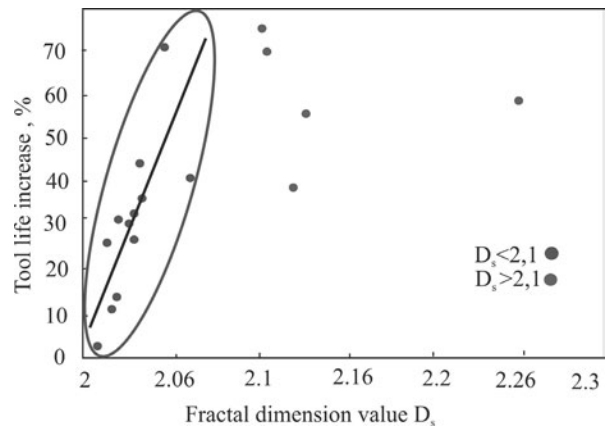


Fig. 7. Dependence of the obtained fractal dimension value and operational properties defined in cutting ability test of coatings obtained in the arc PVD process

## 6. Summary and conclusions

Works [24, 25], presenting structural zones models of coatings point out a fact that structure and topography of coating surface decide their mechanical properties, and consequently, their wear resistance. Employment of the contemporary examination techniques, especially of the scanning electron microscopy [26] and the atomic force microscopy [27], makes observation of coating surface possible, obtained on tool materials with atomic resolution, however, the results are still used only in a limited range. Fractal geometry is a valuable complement to analysis methods for results obtained using the atomic force microscopy [3, 28], rendering it possible to obtain quantitative information characterizing topography of the investigated coatings.

Based on the obtained experimental studies results the of analyses performed, the following conclusions were formulated:

1. In case of coatings obtained in the arc PVD process, prediction of the operational properties defined in the cutting ability test is possible, when the value of their surface fractal dimension  $D_s < 2.1$ . For coatings showing higher  $D_s$  values, predicting the consumer properties on the basis of analysis of the fractal surface topography is encumbered with serious error because of their heterogeneity defined by a high  $\Delta\alpha > 0.47$  value.
2. Growth of the compression stresses values results in the increased coatings' adhesion substrate material (independent from deposition process type).
3. It was indicated in this paper that texture is the crucial factor, deciding not only the mechanical and service properties, but also influencing the surface topography of coatings obtained in the PVD and CVD processes. This aspect requires further investigations for coatings showing distinct differences in terms of their privileged growth orientation type.

## Additional information

Selected issues related to this paper were presented at the 18<sup>th</sup> International Scientific Conference on Achievements in Mechanical and Materials Engineering AMME' 2010.

## References

- [1] W. Kwaśny, M. Woźniak, J. Mikula, L.A. Dobrzański, Structure, physical properties and multifractal characteristics of the PVD and CVD coatings deposition onto the  $Al_2O_3+TiC$  ceramics, *Journal of Computational Materials Sciences and Surface Engineering* 1 (2007) 97-113.
- [2] W. Kwaśny, L.A. Dobrzański, Structure, physical properties and fractal character of surface topography of the Ti+TiC coatings on sintered high speed steel, *Journal of Materials Processing Technology* 164-165 (2005) 1519-1523.
- [3] W. Kwaśny, L.A. Dobrzański, M. Pawlyta, W. Gulbiński, Fractal nature of surface topography and physical properties of the coatings obtained using magnetron sputtering, *Journal of Materials Processing Technology* 157-158 (2004) 183-187.
- [4] B.B. Mandelbrot, Multifractal measures, especially for the geophysicist, *Pure and Applied Geophysics* 131 (1989) 5-42.
- [5] B.B. Mandelbrot, D.E. Passoja, A.J. Paullay, Fractal character of fracture surfaces of metals, *Nature* 308 (1984) 721-722.
- [6] X. Wang, H. Zhou, Z. Wang, M. Tian, Y. Liu, Q. Kong, Fractal analysis of cyclic creep fractured surfaces of two high temperature alloys, *Materials Science and Engineering A* 266 (1999) 250-254.
- [7] A. Celli, A. Tucci, L. Esposito, P. Carlo, Fractal analysis of cracks in alumina-zirconia composites, *Journal of the American Ceramic Society* 23 (2003) 469-479.
- [8] S. Stach, J. Cybo, J. Cwajna, S. Rozkosz, Multifractal description of fracture morphology. Full 3D analysis of a fracture surface, *Materials Science* 23/2 (2005) 577-584 (in Polish).
- [9] C.H. Shek, G. M. Lin, K.L. Lee, J. K. L. Lai, Fractal fracture of amorphous Fe Ni V Si B alloy, *Journal of Non-Crystalline Solids* 224 (1998) 244-248.
- [10] A. Provata, P. Falaras, A. Xagas, Fractal features of titanium oxide surfaces, *Chemical Physics Letter* 297 (1998) 484-490.
- [11] S.L. Mills, G.C. Lees, C.M. Liauw, S. Lynch, Dispersion assessment of flame retardant filler/polymer systems using a combination of X-ray mapping and multifractal analysis, *Polymer Testing* 21 (2002) 941-948.
- [12] M.A. Lebyodkin, Y. Estrin, Multifractal analysis of the Portevin-Le Chatelier effect: General approach and application to AlMg and AlMg /Al<sub>2</sub>O<sub>3</sub> alloys, *Acta Materialia* 53 (2005) 3403-3413.
- [13] C.R. Neto, K. Bube, A. Cser, A. Otto, U. Feudel, Multifractal spectrum of a laser beam melt ablation process, *Physica A* 344 (2004) 580-586.
- [14] D. Chapard, I. Degasne, G. Hure, E. Legrand, M. Audran, M.F. Basle, Image analysis measurements of roughness by texture and fractal analysis correlate with contact profilometry, *Biomaterials* 24 (2003) 1399-1407.
- [15] J.L. Drummond, M. Thompson, B.J. Super, Fracture surface examination of dental ceramics using fractal analysis, *Dental Materials* 21 (2005) 586-589.
- [16] K. Pawlik, Determination of the Orientation Distribution Function from Pole Figures In Arbitrarily Defined Cells, *Physica Status Solidi B* 134 (1986) 477-483.
- [17] W. Kwaśny, A modification of the method for determination of the surface fractal dimension and multifractal analysis, *Journal of Achievements in Materials and Manufacturing Engineering* 33/2 (2009) 115-125.
- [18] S. Chowdhury, M.T. Laugier, J. Henry, XRD stress analysis of CVD diamond coatings on SiC substrates, *International Journal of Refractory Metals & Hard Materials* 25 (2007) 39-45.
- [19] K. Van Hacker, L. De Buyser, J.P. Celis, P. Van Houtte, Characterization of thin nickel electrocoatings by the low-angle diffraction method, *Journal of Applied Crystallography* 27 (1994) 56-66.
- [20] C. Quaeys, G. Knuyt, L.M. Stals, Study of the residual macroscopic stress in TiN coatings deposited on various steel type, *Surface and Coatings Technology* 74-75 (1995) 104-109.

- [21] S.J. Skrzypek, New Approach to Measuring Residual Macro-Stresses with the Application of the Grazing Angle X-Ray Diffraction Geometry, Scientifically Didactic College Publishing House, Cracow, 2002.
- [22] A. Baczmanski, C. Braham, W. Seiler, N. Shiraki, Multi-reflection method and grazing incidence geometry used for stress measurement by X-ray diffraction, Surface and Coatings Technology 182 (2004) 43-54.
- [23] P. Cichosz, Cutting Tools, WNT, Warsaw, 2006 (in Polish).
- [24] J.A. Thornton, The microstructure of sputter-deposited coatings, Journal of Vacuum Science Technology A 4 (1986) 3059-3065.
- [25] B.A. Movchan, A.V. Demchishin, Fizika Metallov i Metallovedenie 28 (1969) 653-656.
- [26] L.A. Dobrzański, J. Mięka, The structure and functional properties of PVD and CVD coated  $\text{Al}_2\text{O}_3 + \text{ZrO}_2$  oxide tool ceramics, Journal of Materials Processing Technology 167 (2005) 438-446.
- [27] Z.-J. Liu, P.W. Shum, Y.G. Shen, Surface growth of (Ti,Al)N thin films on smooth and rough substrates, Thin Solid Films 496 (2006) 326-332.
- [28] Y. Jin, W. Wu, L. Li, J. Chen, J. Zhang, Y. Zuo, J. Fu, Effect of sputtering power on surface topography of dc magnetron sputtered Ti thin films observed by AFM, Applied Surface Science 255 (2009) 4673-4679.